technologies

MDPI

Article

CAD Analysis of 3D Printed Parts for Material Extrusion—Pre-Processing Optimization Method

Andrei Mario Ivan *, Cozmin Adrian Cristoiu and Lidia Florentina Parpala

Faculty of Industrial Engineering and Robotics, National University of Science and Technology Politehnica București, Splaiul Independentei No. 313, 060042 Bucharest, Romania; cozmin.cristoiu@upb.ro (C.A.C.); lidia.parpala@upb.ro (L.F.P.)

* Correspondence: andrei_mario.ivan@upb.ro

Abstract

Free form fabrication (FFF), also known as fused deposition modeling (FDM), is a widespread and accessible method for prototyping. Parts a with lattice structure having functional roles as mechanism elements is becoming more common. In the research field, the mechanical characteristics as well as optimization methods for manufacturing these parts are major points of interest. One of the major aspects of FFF is part orientation during print, as it has influence over a wide range of variables, from tensile strength to surface quality and material consumption. For parts with a lattice structure, the printing orientation is important not only as a factor that influences the characteristics of the part itself, but also as a factor that determines the support requirements. However, due to the complex lattice structure, removing supports from these parts can be a challenging task. This study focuses on analyzing the reliability of available CAD optimization methods for FFF pre-processing. The analysis is performed using the Design for Additive Manufacturing module included in the Siemens NX software, version NX2406. The efficiency of CAD optimization was observed by taking into account the material consumption, printing times, surface quality, and support requirements. The study methods were based on the comparative analysis approach. The case studies used for the comparative analysis consider two-part inner structures: the solid structure approach with a rectilinear infill and the lattice structure approach.

Keywords: FFF; material extrusion; CAD optimization; 3D print; lattice structures

check for updates

Academic Editor: Haijun Gong

Received: 16 July 2025
Revised: 28 August 2025
Accepted: 31 August 2025
Published: 3 September 2025

Citation: Ivan, A.M.; Cristoiu, C.A.; Parpala, L.F. CAD Analysis of 3D Printed Parts for Material Extrusion—Pre-Processing Optimization Method. *Technologies* **2025**, *13*, 398. https://doi.org/10.3390/technologies13090398

Copyright: © 2025 by the authors. Licensee MDPI, Basel, Switzerland. This article is an open access article distributed under the terms and conditions of the Creative Commons Attribution (CC BY) license (https://creativecommons.org/licenses/by/4.0/).

1. Introduction

Originally a prototyping technology, 3D printing has evolved to manufacture various parts with functional or decorative roles in specific applications. Today, 3D printing is suitable for both prototyping and manufacturing functional parts due to its ability to create personalized and complex models [1]. Among 3D printing processes, material extrusion (ME) occupies a well-defined spot, as noted by Jandyal et al. [2]. Some parts are difficult to produce using conventional manufacturing processes due to high costs, which are driven by the required tools and equipment, long production times, and prohibitive material waste. Over time, ME has been integrated into numerous industrial areas and is now used in medical engineering (for personalized prostheses and orthoses), the automotive industry (for jigs and fixtures), the aerospace industry (for lightweight parts with internal channels for cooling and fluid flow), and many others [3,4]. Although selective laser sintering

of metal powders is usually implemented for moving parts [5], prototype parts are still necessary in various fields, where ME remains the most convenient solution [6].

Besides their role in rapid prototyping, parts manufactured using the ME technology gained more and more ground in the field of functional parts used as final products in various applications [7]. New advances in ME (and generally in AM) allow for the produced parts to be suitable for industries such as automotive and aerospace [8]. Furthermore, the development of the Design for Additive Manufacturing set of guidelines shows that this area is indeed a dynamic one and the emergence of ME as a final product manufacturing technology is of major concern in both the research field and in industry. The main obstacles in this development direction are the large anisotropy of the structures obtained through FFF and the mechanical properties of the parts [9,10]. Thus, process study and optimization are essential to the development of ME technology in this direction.

Regardless of the technology or materials used, several objectives regarding process optimization should be considered, such as reducing printing times, minimizing filament consumption, avoiding the need for supports, and achieving a higher surface and structural quality of the part [11,12]. In practice, many issues affect these aspects, including stringing, warping, layer shifting, inconsistent extrusion, ghosting, layer separation, bed adhesion, and structural or shape issues caused by coding or modeling errors [13,14].

The advantages of the ME approach for producing parts in various fields are well documented in the literature. Tofail et al. highlighted the general advantages of additive manufacturing, while also discussing the challenges related to process complexity, the large number of variables, and the repeatability of results [15]. In their review, Jandyal et al. highlighted poor mechanical performance as one of the main disadvantages of FFF [2]. These low-level mechanical properties have been linked to the internal structures of the parts. Aloyaydi et al. studied the influence of the infill pattern on the tensile strength of the parts and found that the grid pattern generated the highest tensile strength, as the layers are arranged in alternating orientations [16].

The influence of various ME process parameters on the mechanical properties of 3D printed parts has also been studied by numerous researchers [17–21]. Many of these studies show that orientation during printing is a major factor influencing part characteristics and mechanical properties. Giri et al. obtained results showing the influence of part orientation during material deposition on the tensile strength of the part in correlation with printing time and layer thickness [22]. Raju et al. demonstrated that part orientation affects several mechanical characteristics, such as hardness, tensile strength, and flexural modulus [23]. Górski et al. found a correlation between layer orientation, loading force direction, and material strength [24], ultimately emphasizing the importance of part orientation during printing. These results are consistent with those obtained by Hernandez et al. [25].

It is evident that one of the main disadvantages of the ME approach—the mechanical properties of parts—is extensively studied in the literature. Therefore, part orientation during printing is a major concern for the pre-processing optimization of FFF.

In ME, lattice structures are used to improve the structural characteristics of parts in multiple directions [26]. These types of structures typically result in lightweight parts, which are essential in the automotive and aerospace industries where a lower mass leads to reduced energy requirements [27]. The lattice geometry allows for the directional adjustment of mechanical properties through structural optimization, making it useful for various applications and working parameters. It also influences the thermal properties of the part, allowing for better heat dissipation or insulation as needed [28].

The materials used (metallic or polymer powders), together with the lattice design, determine the properties of the final part and allow for a higher level of customization of its characteristics; however, these properties can still be compromised by geometric flaws

and printing errors. For example, a flaw in the designed lattice structure could alter the porosity, which in turn affects the mechanical and thermal properties of the part [29]. Some of these issues can be adjusted through machine calibration or printing parameters. Others require a 3D printability analysis using specific software applications or modules.

It is worth noting that the process optimization is essential in the development of ME technology and represents a major research direction in the field. Some of the main areas of concern, especially regarding 3D printed parts intended as final products, are linked to the mechanical properties. For this, various works have shown that lattice structures might be the answer. On the other hand, process optimization solutions can be implemented before print (pre-processing), during print, and after the print is completed (post-processing). Generally speaking, the pre-processing optimization approach is based on several elements, including part geometry and orientation. Some of the pre-processing optimization methods employ the use of CAD optimization modules to analyze the part and suggest the best print orientation. Although these CAD modules—such as the Design for Additive Manufacturing module included in the Siemens NX software (version NX2406)—have the potential to offer better solutions for ME processes, there are no studies in the literature that evaluate their efficiency and applicability.

For parts that have a lattice structure, one of the issues is linked to the supports' requirements, as the complex structure makes removing these supports difficult. Adding the fact that printing supports increase material consumption and printing times, finding a solution that has the potential to reduce the use of supports in FFF would significantly contribute to process optimization.

Considering the aspects presented above, the main goal of this work is to use the comparative analysis method to validate the CAD optimization approach for ME. The main criterion for validation is filament consumption, with a focus on the support material. Since the Design for Additive Manufacturing module uses geometric criteria for part posture optimization, focusing on support requirements, overhangs reduction, and material consumption, the printing parameters taken into consideration are those that are directly linked to the software module criteria, since the research evaluates the efficiency of the software, and the analysis is focused on the improvements that the software claims to provide. Furthermore, the research aims to evaluate the level of improvement that the software brings to the printing process when considering the analyzed criteria. Thus, the study aims at reducing support requirements for parts obtained through the ME method using CAD optimization tools. This comparative analysis is performed using data from the slicer and experimental results obtained using two different part inner structures. Taking into account the optimization criteria used by the software module and the corresponding parameters of the printing process and the printed part (the parameters that are directly linked to the optimization criteria of the software), the following factors were included in the analysis: support weight, total part weight, print duration, amount of post-processing required, and surface quality. The specified parameters together define the scope of the research. The results will evaluate the efficiency of the software for the pre-processing analysis together with the influence on process optimization and print quality. While mainly focusing on reducing the support material requirements, the study also takes into account other factors, such as the surface quality of the printed part, printing time, and total material consumption. Including these factors into the analysis was necessary in order to assess the support material requirement in the larger context of FFF and to provide a robust evaluation. The article is structured as follows:

- The second chapter will review the state of the art regarding FFF, focusing on the latest approaches.
- The third chapter will include two case studies on the optimal printing orientation. The first case study was performed on the solid structure of the part with a rectilinear

infill configured in the slicer, while the second case study was performed on the same part with lattice structure.

- The fourth chapter will explore the proposed CAD analysis methods required for preparing the ME process. This chapter will also include experimental data obtained through applying the proposed analysis methods to the ME processes. The main method of evaluation used is a comparative analysis. The main criteria for the analysis are support volume and mass, material consumption, printing times, and surface quality.
- The last chapter will focus on the conclusions drawn, including future research directions.

2. State of the Art

FFF has experienced rapid growth and development in recent years, leading to an increase in the quality of manufactured parts and the efficiency of the process itself. As a result, optimizing printing parameters has become a focal point in research. The main goal of this optimization is to improve the mechanical and aesthetic properties of the printed parts. The quality of the parts is influenced by several factors:

- Process parameters: These include printing temperature, extrusion speed, layer height, printing speed, and bed temperature.
- Part design: The shape and dimensions of the part influence the preparation method, the process itself, and the printing results.
- Material: The type of material used for 3D printing affects the physical and mechanical properties of the part.

Taking these aspects into account, some of the latest research is oriented towards optimizing printing parameters to customize the mechanical properties of printed parts, such as tensile strength, compressive strength, flexural strength, impact strength, and hardness. One solution to these issues is the multi-objective optimization method, which can optimize parameters related to mechanical characteristics and production costs [30]. In a recent study, Zisopol et al. demonstrated that the optimal values for the mechanical properties of printed parts can be experimentally determined by adjusting the layer height and infill parameters [30].

Another main research direction focuses on improving the aesthetic properties of 3D-printed parts. A recent study by Jackson et al. [31] identified the effects of the retraction speed, filament deposition angle, and the number of layers and walls. This work also showed that by optimizing the retraction speed, the maximum tensile strength of the part could be improved by up to 15%. It was observed that the retraction speed, together with the deposition angle, have a major influence on the quality of part surfaces.

In addition to improving the physical properties of printed parts, the literature also includes works on optimizing energy consumption and printing times. El Youbi El Idrissi et al. [32] used machine learning algorithms trained with data obtained through the r3DiM benchmark [33], identifying the influence of part printing orientation on energy consumption and printing times.

The necessity of part customization for specific applications with particular requirements has also led to research on 3D printing materials. Besides the usual ABS, PET, PLA, and PETG, other filament types have been developed, including composite materials such as CFRTPC (continuous fiber-reinforced thermoplastic composites). These composite materials have special properties related to corrosion and fatigue resistance [34], making them suitable for use in the aerospace and nuclear industries. The equipment and printing technology used for these materials differs from conventional 3D printing setups, and the development of such systems constitutes another point of interest in research in this field.

Usually, the heat required for melting the filament is generated using the electrical resistance principle. However, Li et al. [35] developed a printing method that uses microwaves for this purpose. This method, which allows for more efficient heating, showed that the filament thickness could be increased to 5.5 mm and the printing speed could be increased by over three times.

Recent results strengthen the link between lattice architecture/orientation and performance. Liu et al. [36] introduce a twin-oriented design for TPMS lattice metamaterials and report an enhanced super-elastic response, load-carrying capacity, energy absorption, and improved fatigue behavior by aligning the lattice orientation with the load paths, highlighting that the cell architecture plus orientation co-determine fatigue resistance. Complementarily, Numan and Aniello [37] present a systematic review of aerospace lattice structures, mapping a current design for additive manufacturing trends (graded and TPMS lattices, multifunctional optimization), fatigue-aware design rules, and open directions for lightweight components, underscoring the central role of orientation and overhang management in both performance and post-processing.

Precision and dimensional stability of the parts are other important aspects of the 3D printing process. By using different analysis and predictive methods, Min et al. [38] anticipated the dimensional errors of the printed parts with a precision of several microns. The analysis took into account factors such as filament deposition angle, layer thickness, and different support materials.

While most research in the field focuses on the printing process, materials, or equipment, there are far fewer studies that consider CAD modeling as an integral part of a successful printing process. Although CAD modeling might not seem directly linked to the 3D printing process itself, optimizing the geometry of the part while maintaining its physical and aesthetic specifications is crucial, as it greatly influences the printing process. For this reason, the following case study demonstrates a method of anticipating potential printing errors and determining solutions for optimal part geometry, positioning, and orientation, leading to lower filament consumption (especially support material) and reduced printing times.

The presented study is linked to the research performed by the authors in the field of FFF, especially focused on optimizing the printing parameters and pre-processing procedures. The CAD optimization used for analysis was also implemented to determine the optimal printing orientation for a part with a relatively simple shape. However, the experimental data showed that, while the posture provided by the CAD analysis tool provided the best results, some of the standard part orientation solutions configured using the slicer generated comparable outcomes. Furthermore, parts with a rectangular shape and wide planar surfaces that could be placed flat on the printing bed benefit from more standard orientation solutions that often require no supports. The aspect of minimizing the supports' requirements (which is recognized as an important issue in the literature) is harder to manage in the case of parts with more complex shapes: more curvatures, round or irregular surfaces, etc. In these cases, more careful planning in the pre-processing stage is required. Furthermore, parts with a lattice structure require more management regarding supports due to the complex geometry and difficulties in removing the extra material.

3. Materials and Methods

In order to perform the analysis and reach the proposed objectives, a part that resembles a brake pedal was used. This sample was chosen because it aggregates features that are known to drive support demand in FDM: overhangs, mixed flat/curved surfaces, varying cross-sections/fillets, and the option to realize the same external envelope with either a solid or a lattice interior. This combination makes purely planar or axis-aligned

placements sub-optimal and stresses the need for upstream orientation screening. The orientation benefit observed here extends to other classes of parts with overhang-driven morphology, for example: topological optimized brackets used in automotive [39], panels with exposed lattice skins for aerospace [37] (tilts that render lattice struts self-supporting reduce support contact and cleanup), medical implants [40], hollow ducts/elbows with internal channels [41] (orientations that keep the channel roof within the self-support angle avoid non-removable internal supports) etc. These examples of part types are shown in Figure 1.



Figure 1. Types of parts for which print orientation optimization is suitable.

The study was conducted using two models of the part. The first model had a solid inner structure, while the second model had a lattice structure. For 3D printing, the first model was configured in the slicer with a rectilinear infill of 20%. For the second model, the lattice structure itself was considered as the inner configuration of the part. The parts were printed using Polyterra PLA manufactured by Polymaker (Changshu, China). The printing was done on a Creality Ender 3 V2 Neo machine manufactured by Creality (Shenzen, China).

In the context of this study, the posture of the part during print was considered to fall into one of the following two categories: standard orientation or optimized orientation. Standard orientation was considered as any of the postures obtained from slicers by selecting one of the major flat surfaces of the part and aligning it to the build plate. Alternatively, in the case of more complex shaped parts, the postures that aligned the major surfaces of the object in vertical positions were considered as falling into the standard category. In many situations, this posture relies heavily on a visual inspection of the part and on user experience. The optimized orientation was obtained from the analysis performed using the dedicated CAD software (included in version NX2406). Our CAD-first orientation screening is consistent with the FDM dimensioning/orientation guidelines that recommend defining the printing reference plane and building direction explicitly to avoid support-driven artifacts and stabilize dimensional outcomes [42]

The analyzed part is shown in Figure 1 with the solid structure. The surfaces and alignment lines used to determine the standard orientations for 3D printing are identified in Figure 2. The lattice structure of the part is shown in Figure 3. The standard orientations taken into account are illustrated in Figure 4.

The first orientation used for the analysis was determined by placing Surface 3 on the printing bed. In this case, the upper segment of the part (after the curvature) requires supports. The second orientation was determined by aligning Surface 1 with the bed; however, because Surface 4 is wider than the rest of the part, the horizontal body has an overhanging posture and requires supports. The third and the fourth orientations were determined by positioning Surface 1 and Surface 2 vertically. Thus, for the third orientation, the part is placed lying on the bed along Contact line 1, while for the fourth orientation, the part is placed lying on the bed along Contact line 2. In both cases, the underneath surfaces require supports.

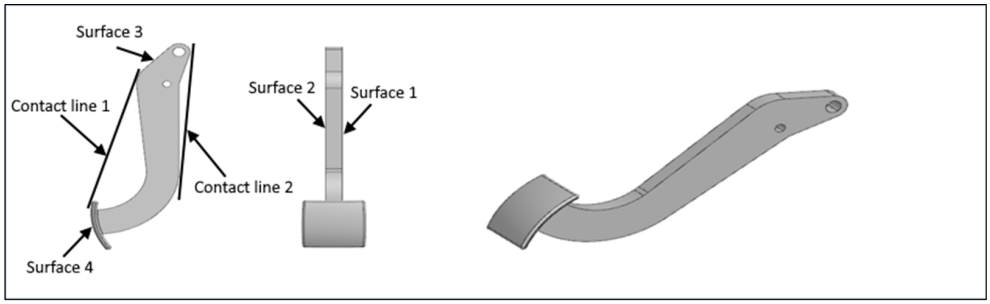


Figure 2. The analyzed part with a solid structure.

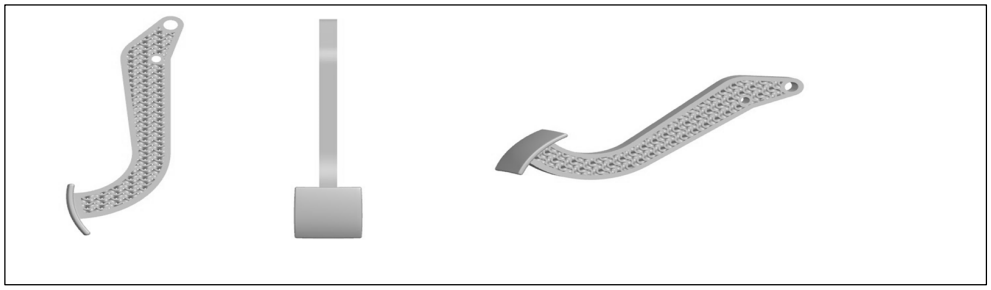


Figure 3. The analyzed part with a lattice structure.

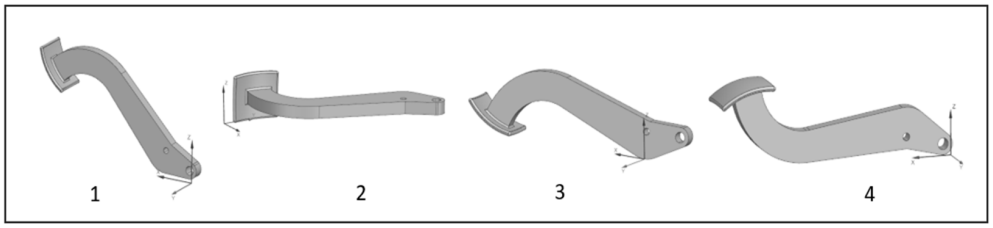


Figure 4. The analyzed standard orientations.

The methodology used to analyze the parts, their orientations during print, and the efficiency of CAD optimization is based on a comparative analysis. First, orientation solutions for both part configurations were established using both the Prusa slicer (version 2.8.1) and the Design for Additive Manufacturing module included in the Siemens NX software (version NX2406). The printing data estimations from the slicer and the CAD software (NX2406) were noted and compared. All the parts were printed using the specified orientations on the same printer, with the same general printing parameters. After printing, the total mass of the part was measured in each case, together with the mass of the supports and the printing time. The surface quality of the printed parts was also evaluated through a visual inspection. The results were compared in order to observe both the advantages offered by the CAD optimization software and the variation in its efficiency in relation to the complexity of the part.

The software module can be used to analyze different solutions for part orientation during the printing process to optimize printing times and the quantity of the filament used. The software considers three major parameters for optimization: surface area, support volume, and printing time. Also, the user can prioritize one of the parameters over the other two. At the end of the simulation, the 10 best orientation solutions are suggested. For each suggested solution, the surface area, estimated support volume, and printing time data are provided. The command window of the "Optimize Part Orientation" with the least efficient solution is shown in Figure 5. The best solution provided is shown in Figure 6.

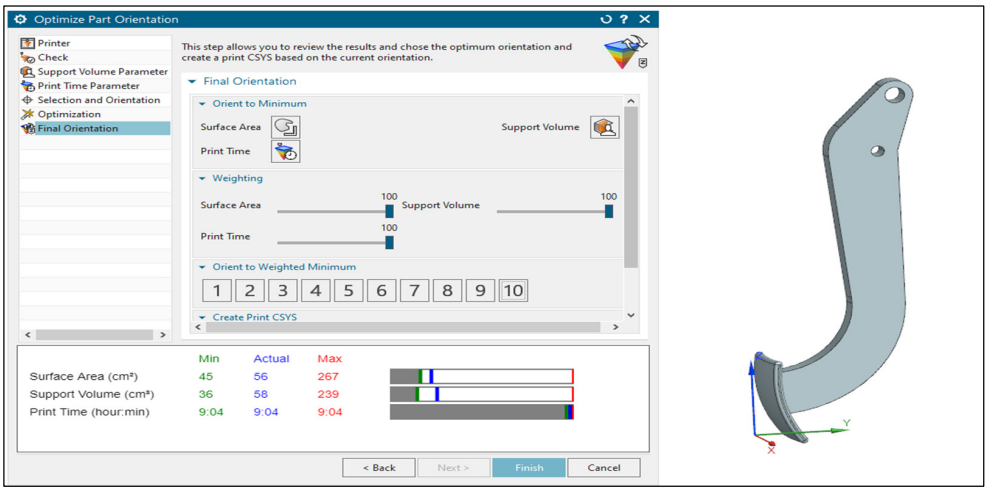


Figure 5. Least efficient solution for part orientation optimization.

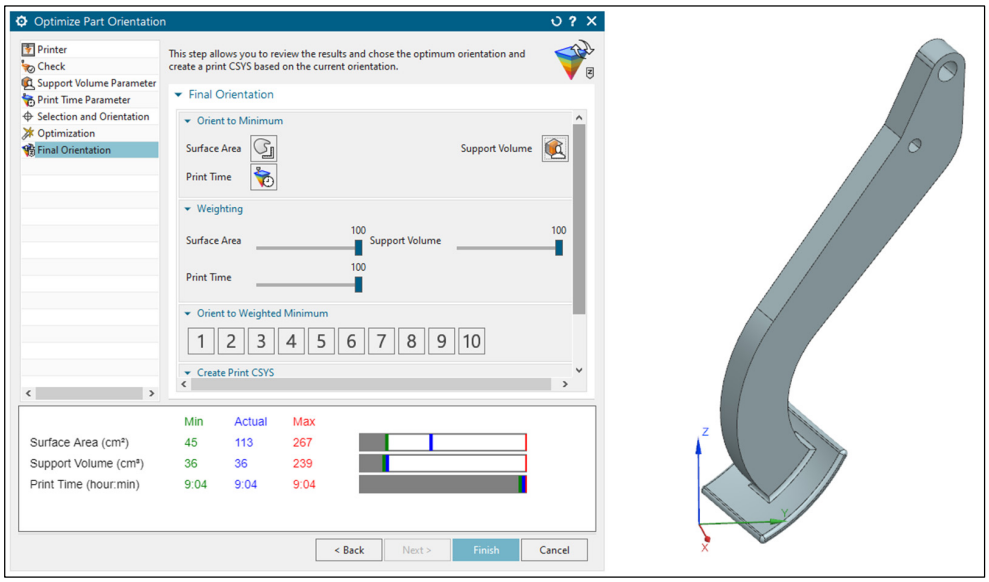


Figure 6. Best solution for part orientation optimization.

Within the Design for Additive Manufacturing module, the "Surface Area" metric denotes the projected footprint of the part on the build plate for a given orientation. It is computed from the faces that are in direct contact with the plate and all the downward-facing faces whose inclination exceeds the user-specified over-hang limit. In other words, it approximates the area that would, in principle, require either direct adhesion or sacrificial support. The "Print Time" value should be interpreted only as a coarse estimate. It is derived from the total build height of the CAD model and a constant material-deposition rate supplied by the user; therefore, candidate orientations with comparable heights often yield identical rounded times. Crucially, the module does not simulate support tool paths, so the additional time associated with support generation is ignored. For this reason, we rely instead on slicer-based estimates and on experimentally measured durations. Finally, "Support Volume" refers to the geometric volume enclosed between the build plate and those over-hang regions that breach the limit angle. It is thus a purely geometric indicator and should not be mistaken for the actual mass/volume of filament required to build the supports.

The analysis showed an optimal printing posture with the part rotated around two axes: a 400 rotation around the X axis and a 100 rotation around the Y axis. This

was considered as an additional part orientation included in the case study, thus increasing the number of analyzed part postures to a total of five. Again, the orientation resulting from the analysis shows major differences when compared with any of the standard orientations. The support volume indicated in this case was 36 cm^3.

Note that the Optimize Part Orientation tool used from NX Software (version NX2406) is an upstream tool, searching positioning and orientation space based on geometric criteria (overhang, surface area, support volume) that are specifically defined in NX (in accordance with the answer provided for the 2nd comment). It helps you to quickly find candidate orientations independent of a specific slicer and allows for the analysis of optimal positions without considering particular placements on the flat faces or orthogonal orientations of the part (unlike slicers). This is the main reason and major benefit: that you can obtain optimal candidate positions and totally unintuitive orientations, such as this tilted positioning of the part in the following Figure 7.

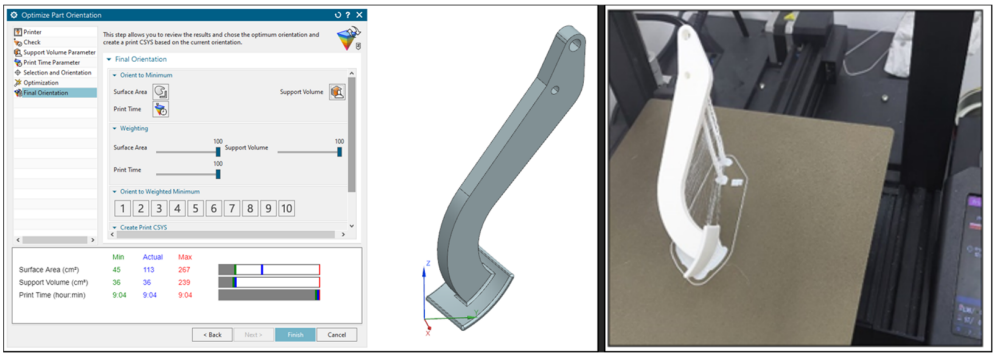


Figure 7. Unintuitive print position provided by NX.

Slicer software (in our case, Prusa Slicer version 2.8.1) is a downstream tool that is machine/profile dependent, which calculates real weights and real times (including support paths) for you after you have chosen an orientation. Usually, these slicers can also provide automatic orientations for parts, but without an optimization analysis, the orientations that are possible to be chosen in these slicers are with the flat surfaces of the part in contact with the printing base or orthogonal orientations, like those in Figure 8.

In the study, NX is not the source of the conclusion; NX only proposes the orientation that minimizes support. The conclusion is drawn from the slicer estimates plus the experimental measurements.

So, the validation method used in this research is experimental. For the CAD analysis, the support volume criterion was prioritized. One of the issues anticipated from the inspection of the solutions proposed by the software is linked to the bed adhesion of the part due to the low contact area with the support surface. Because of the given orientations, printing can prove to be difficult if the machine calibration or the bed surface is not in a very good condition. On the other hand, the advantage of this part orientation is linked to low filament consumption, reduced printing times, reduced post-processing operations, and fewer internal supports, as shown by the CAD analysis estimates. Even with the bed adhesion issues, if filament consumption is an important parameter, the part geometry can be optimized to allow successful printing, and depending on the functional role of the part, chamfers or other support surfaces can be added.

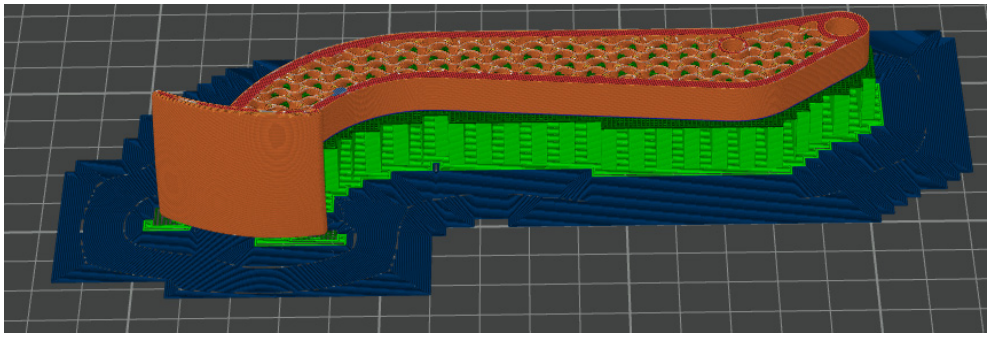


Figure 8. Automatic print orientation provided by the slicer.

The module used to optimize the part orientation for 3D printing has some limitations, such as assuming a 100% infill and a constant printing speed. Additionally, although it can estimate the support material volume required for the analyzed part, it does not consider the time required for printing the supports. Estimating this time would be a useful option, since it depends on various aspects, such as the support structure and different speed values specified in the slicer. Depending on the 3D printer and the slicer used to prepare the G-code file, there are certain aspects regarding the support type and shape, infill model, and different printing speeds for the walls, bottom, and top layers, that influence the filament consumption and printing times. Nevertheless, the analysis approach used in this research remains relevant when considering the corresponding proportions because the optimization regarding filament consumption remains efficient regardless of the printing speed and infill level.

The test part was printed using each of the five proposed orientations twice, once for the solid structure (with infill) and once for the lattice structure. The "PLA PolyTerra" material was used, manufactured by Polymaker (Changshu, China). The properties and specifications of the filament are detailed in the datasheet [43]. The machine used for test printing was a "Creality Ender 3 Neo," a general-purpose 3D printer produced by Creality 3D Technology Co. based in Shenzhen, China. The slicer used was PrusaSlicer version 2.7.4. The settings applied for the tests were as follows:

- Printing speed: 50 mm/s
- Infill speed: 60 mm/s
- Infill pattern: rectilinear
- Layer height: 0.2 mm
- Line width: 0.4 mm
- Printing temperature: 2100
- Build plate temperature: 600
- Retraction speed: 45 mm/s
- Retraction length: 1.2 mm

Since the main objective of the study is lowering the filament consumption, focusing on reducing the support requirements, bed adhesion structures were avoided when possible. Thus, most parts were printed without any brim or raft; however, in cases where printing failed due to poor bed adhesion, such solutions were necessary. For a consistent approach, in each case the supports were automatically generated using the slicer, without manual configuration by the user. The printed parts are shown in Figure 9 for the first part structure and in Figure 10 for the second part structure.

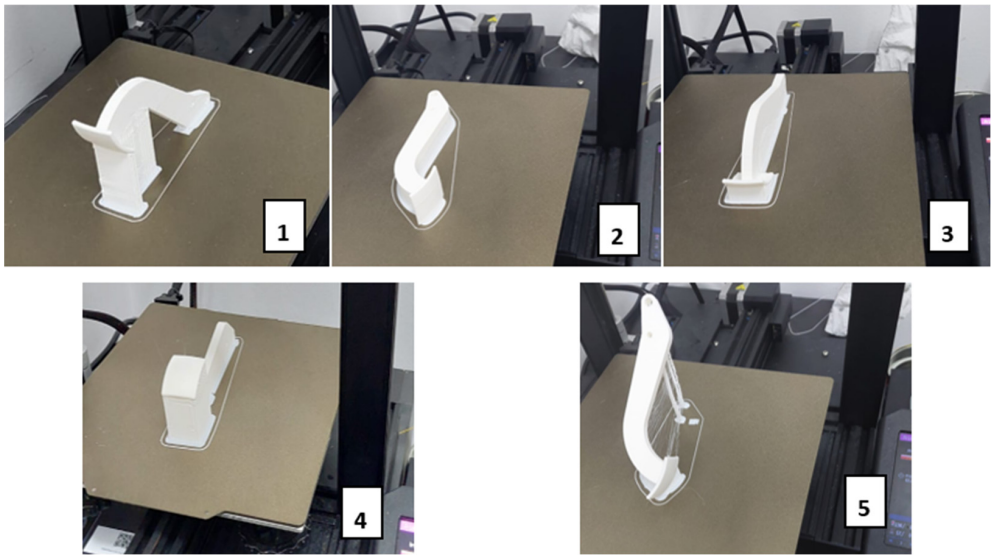


Figure 9. The printed parts using the five proposed orientations—first part structure.

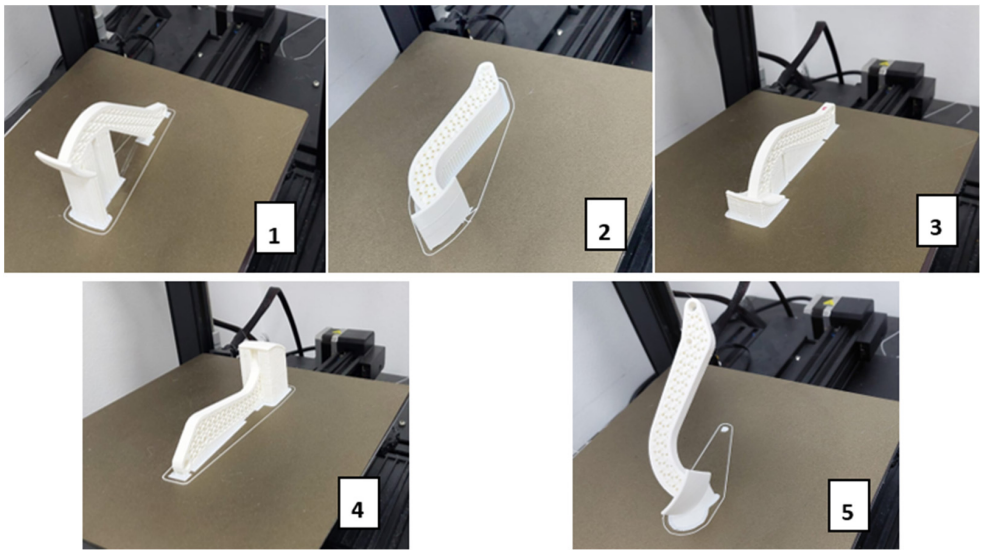


Figure 10. The printed parts using the five proposed orientations—second part structure.

During the case study, the following data were recorded:

- The slicer estimates for the total printed volume, infill level and weight, support weight, print duration, and total weight.
- The experimental data, including total print measured weight, part weight without supports, supports and brim weight, and print duration.
- Furthermore, the quality of the part was assessed through visual inspection. The visual inspection was focused on finding delamination, layer shifting, stair stepping effect, overhang, and other issues.
- For the efficiency analysis, the amount of post-processing required in each case was taken into consideration.

After performing the experimental procedures and collecting the required data, a comparative analysis was used to determine the efficiency of each printing approach. The analysis was based on a mathematical model that determined the score of each printing method for both part structures. The scores were then compared, and the results were used to discuss the outcome.

In order to calculate the efficiency of CAD optimization, each evaluated factor was quantified. The efficiency of each printing setup used was determined by taking into account the weighted value of each factor. Weighing the values of the factors was necessary for a robust and relevant calculation, taking into account the objectives of the research. Thus, the observed parameters were quantified as follows:

- The weight of the supports was determined by weighing the part before and after removing the extra material. Also, the estimated support weight from the slicer was noted. The support weight (expressed in grams), noted with SW, was considered as the base value of this evaluated factor. SW evaluates the support requirements of the corresponding printing orientation and thus was included in the analysis as a direct expression of the optimization criteria used by the software module.
- The total weight of the part was estimated in the slicer before print. Also, the parts were weighted after the operation was completed. It must be noted that the total weight of the part (noted with TW) depends not only on support configuration but also on infill distribution. TW was included in the analysis as an expression of the total material consumption, another optimization criteria used by the software module.
- The print duration was also taken into account (noted with PD). Since the ME process efficiency also depends on productivity, and because from a wider perspective the energy requirements should also be taken into consideration, the print duration (expressed in minutes) influences the outcome of the evaluation. Being an expression of productivity (which influences work efficiency), the print duration was included in the study after observing that the part orientation provided by the software significantly increases the printed height.
- Also linked to process efficiency and productivity, the amount of post-processing required was considered, noted with PPS. This is mainly linked to support material removal, thus being influenced by the support requirements. In order to evaluate the PPS factor, the time (expressed in minutes) required for part post-processing was taken into consideration. For a more precise calculation, the time required for post-processing was expressed using the decimal system, with intervals of 0.5. PPS was included in the analysis because it is a major factor that influences productivity, besides PD.
- Another factor included in the calculation was surface quality, noted with SQS. Effects such as delamination, layer shifting, stair-stepping effect, overhang, etc. were noted. A score of 1 was assigned for each surface that displayed issues that were noticed by visually inspecting the part after printing. For a surface with major issues, a score of 2 was assigned. For a surface with minor issues, a score of 0.5 was assigned. SQS was included in the analysis as one of the aspects that should be improved by the software module used for determining the part printing posture.

Considering the above notations, values, and scores, the efficiency score (ES) of each printed part was calculated. The efficiency score takes into account the support weight value, as it is directly linked to the main goal of the study. The ES shows the efficiency of the corresponding part orientation in the context of the factors that were evaluated. A lower score indicates a more efficient printing posture. The formula for the ES calculation is presented below:

$$ES = a * SW + b * TW + c * PD + d * PPS + e * SQS$$

where a, b, c, d, and e are coefficients that are used to adjust the elements of the formula. For the formula, all the values were converted to dimensionless quantities.

These coefficients are required for two main reasons:

- The parameters have different value ranges. For example, typically the PD parameter (expressed in minutes) will have a much higher value than the part weight (expressed in grams), since the material flow rated in a standard FDM process is much greater than 1 g/min. This, in turn, can affect the formula efficiency, since the PD parameter will have a greater influence on the final score. To compensate for this issue, the coefficients can be used to scale the formula elements to more comparable values.
- The coefficients can also be used as adjustment tools for the formula, giving it greater flexibility. Since the analyzed parameters are more or less relevant, depending on the characteristics of the performed study, the coefficients can be modified to alter the weight of the parameters according to each study's requirements. Thus, the formula can be adapted and used for other research projects or optimization procedures.

4. Results and Discussions

The estimated data supplied by the slicer, as well as the data gathered from measuring and analyzing the 3D printed parts and the process itself, were taken into account and included in the comparative analysis. Table 1 shows the estimated data extracted from the slicer for the first part structure. Table 2 shows the estimated data extracted from the slicer for the second part structure. The data provided by the slicer refer to the support weight, total weight, and print duration parameters. The post-processing score and surface quality score are based on a visual inspection of the part. Thus, these scores were not taken into consideration for the slicer estimates. For the experimental measurements data (Tables 3 and 4), PPS and SQS have values that are determined using the rules stated above: PPS is an expression of the time required for part post-processing (expressed in minutes using the decimal system, with intervals of 0.5) and SQS is an expression of the number of surfaces with visible issues (normally, a score of 1 is assigned for each surface with issues; a surface with major issues has a score of 2; and a surface with minor issues has a score of 0.5).

Table 1. Slicer data—first part structure.

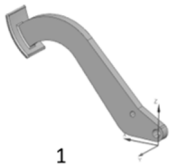
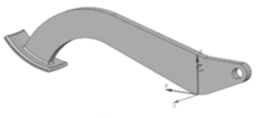
 1	Support weight SW [g]	5.84
	Total weight TW [g]	21.12
	Print duration PD [min]	146
	Post-processing score PPS	-
	Surface quality score SQS	-
 2	Support weight SW [g]	9.58
	Total weight TW [g]	22.14
	Print duration PD [min]	96
	Post-processing score PPS	-
	Surface quality score SQS	-
 3	Support weight SW [g]	4.77
	Total weight TW [g]	20.02
	Print duration PD [min]	135
	Post-processing score PPS	-
	Surface quality score SQS	-

Table 1. *Cont.*

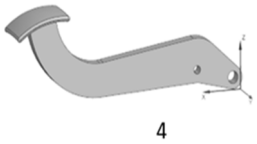
 4	Support weight SW [g]	9.2
	Total weight TW [g]	24.6
	Print duration PD [min]	145
	Post-processing score PPS	-
	Surface quality score SQS	-
 5	Support weight SW [g]	0.4
	Total weight TW [g]	16.27
	Print duration PD [min]	171
	Post-processing score PPS	-
	Surface quality score SQS	-

Table 2. Slicer data—second part structure.

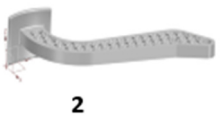
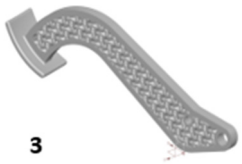
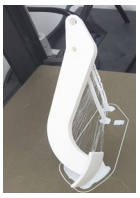
 1	Support weight SW [g]	7.96
	Total weight TW [g]	23.61
	Print duration PD [min]	192
	Post-processing score PPS	-
	Surface quality score SQS	-
 2	Support weight SW [g]	9.16
	Total weight TW [g]	24.68
	Print duration PD [min]	186
	Post-processing score PPS	-
	Surface quality score SQS	-
 3	Support weight SW [g]	5.76
	Total weight TW [g]	21.01
	Print duration PD [min]	195
	Post-processing score PPS	-
	Surface quality score SQS	-
 4	Support weight SW [g]	9.28
	Total weight TW [g]	24.44
	Print duration PD [min]	197
	Post-processing score PPS	-
	Surface quality score SQS	-
 5	Support weight SW [g]	0.76
	Total weight TW [g]	16.36
	Print duration PD [min]	196
	Post-processing score PPS	-
	Surface quality score SQS	-

Table 3. Experimental measurements data—first part structure.

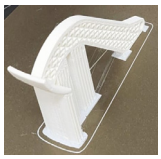
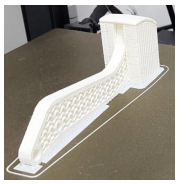
	Support weight SW [g]	6.29
	Total weight TW [g]	22.14
	Print duration PD [min]	135
	Post-processing score PPS	4
	Surface quality score SQS	3.5
	Support weight SW [g]	9.91
	Total weight TW [g]	22.09
	Print duration PD [min]	107
	Post-processing score PPS	5
	Surface quality score SQS	3
	Support weight SW [g]	3.78
	Total weight TW [g]	20
	Print duration PD [min]	147
	Post-processing score PPS	6.5
	Surface quality score SQS	5
	Support weight SW [g]	8.69
	Total weight TW [g]	24.68
	Print duration PD [min]	167
	Post-processing score PPS	8
	Surface quality score SQS	5
	Support weight SW [g]	0.54
	Total weight TW [g]	16.2
	Print duration PD [min]	185
	Post-processing score PPS	1
	Surface quality score SQS	0.5

After the printing was performed, the weight of the part was measured both including and without the supports. The printing time as indicated by the printer was noted for each part. Furthermore, the surface quality and the post-processing requirements were analyzed, and the corresponding scores were assigned. Table 3 shows the experimental data for the first part structure, while Table 4 shows the experimental data for the second part structure.

In order to offer a better perspective and to perform a visual comparison between the values estimated by the slicer and the values obtained through experimental procedures, the data for the support weight, total part weight, and print duration were graphically analyzed using bar charts. The data for the first part structure are displayed in Figure 11 (support weight SW), Figure 12 (total part weight TW), and Figure 13 (print duration PD). The data for the second part structure is displayed in Figure 14 (support weight SW), Figure 15 (total part weight TW) and Figure 16 (print duration PD).

A comparative analysis in graphic form was also performed on the post-processing score PPS and surface quality score SQS of the first- and second-part structure. The score comparison for the post-processing score is illustrated in Figure 17. The score comparison for the surface quality score is illustrated in Figure 18.

Table 4. Experimental measurements data—second part structure.

	Support weight SW [g]	8.85
	Total weight TW [g]	24.83
	Print duration PD [min]	179
	Post-processing score PPS	4
	Surface quality score SQS	3.5
	Support weight SW [g]	9.94
	Total weight TW [g]	24.77
	Print duration PD [min]	171
	Post-processing score PPS	13
	Surface quality score SQS	7
	Support weight SW [g]	5.41
	Total weight TW [g]	20.36
	Print duration PD [min]	188
	Post-processing score PPS	6.5
	Surface quality score SQS	5
	Support weight SW [g]	10.15
	Total weight TW [g]	24.8
	Print duration PD [min]	188
	Post-processing score PPS	8
	Surface quality score SQS	5
	Support weight SW [g]	0.43
	Total weight TW [g]	11.23
	Print duration PD [min]	195
	Post-processing score PPS	1
	Surface quality score SQS	0.5

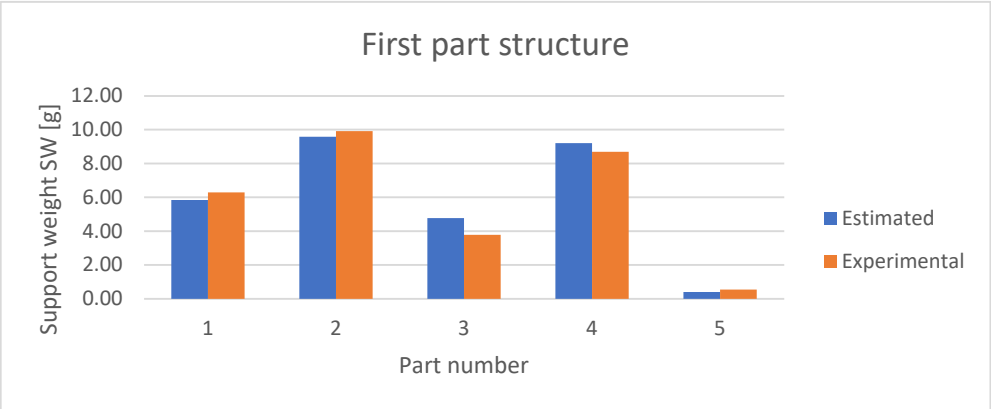


Figure 11. Support weight comparison—first part structure.

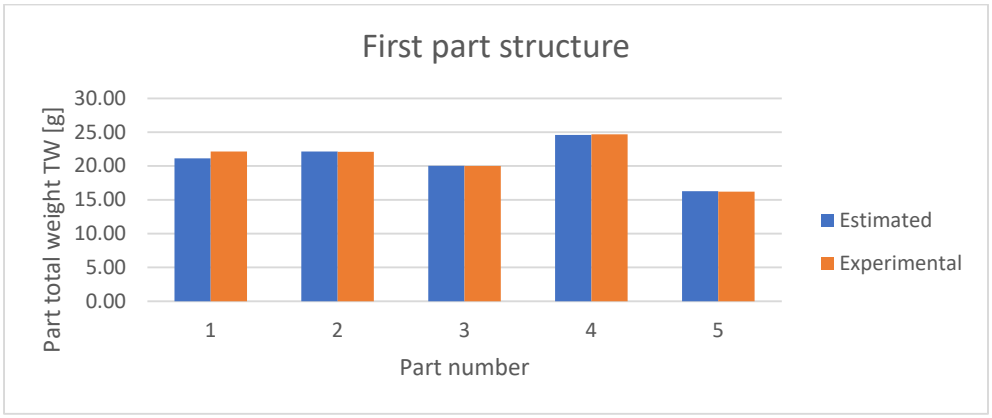


Figure 12. Part total weight comparison—first part structure.

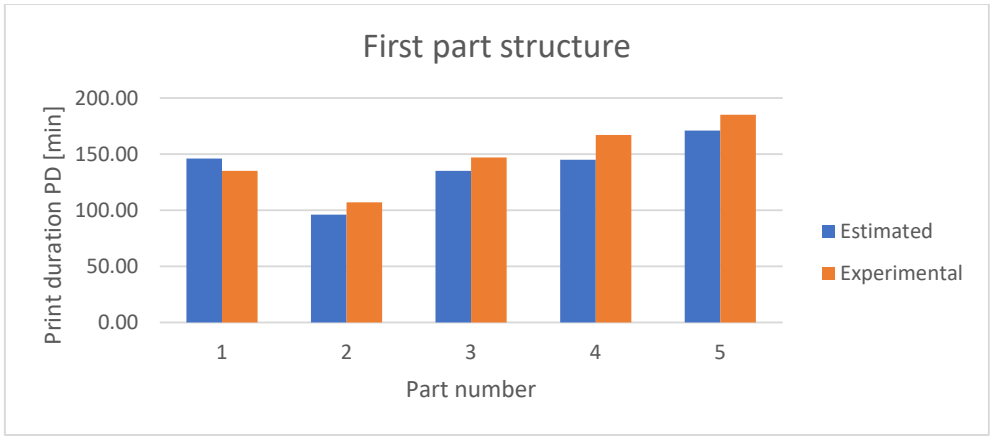


Figure 13. Printing time comparison—first part structure.

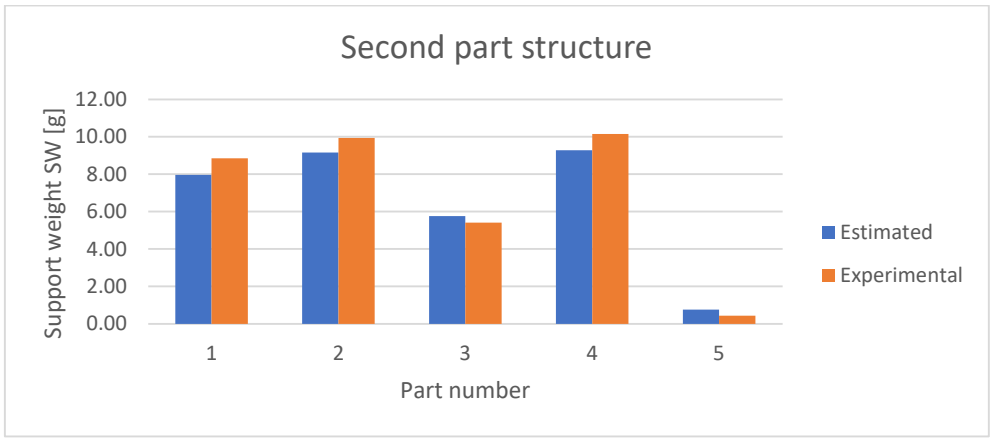


Figure 14. Support weight comparison—second part structure.

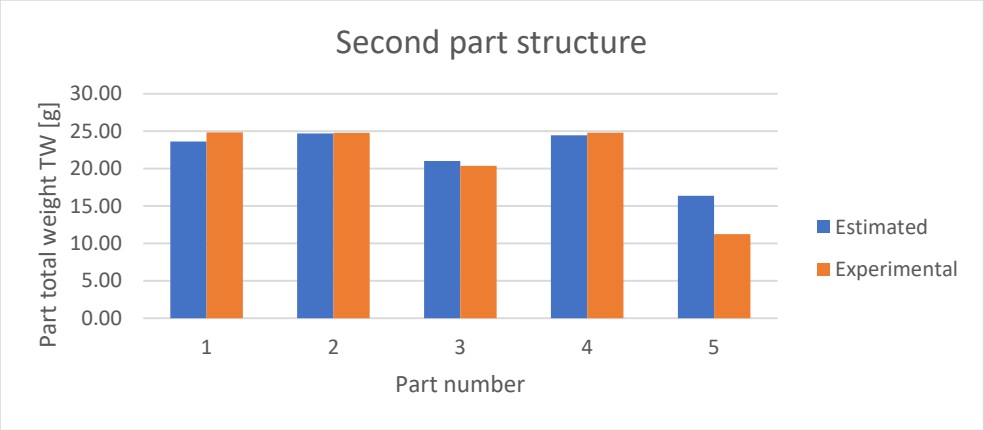


Figure 15. Part total weight comparison—second part structure.

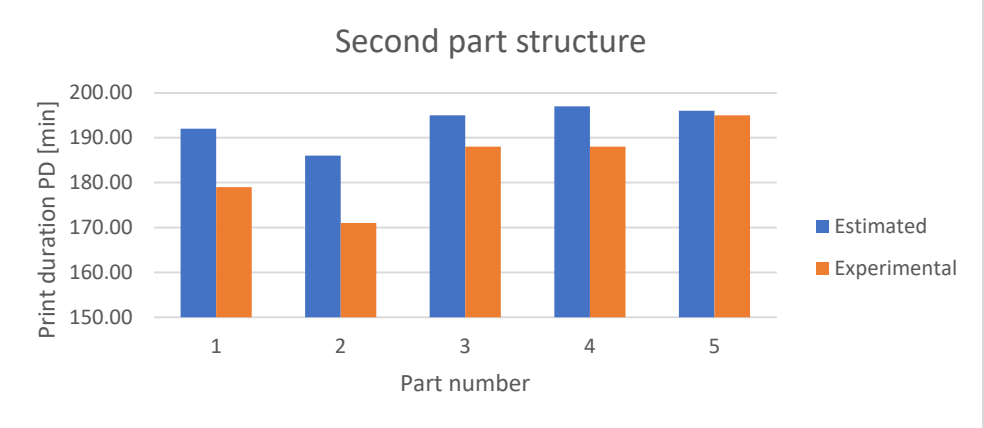


Figure 16. Printing time comparison—second part structure.

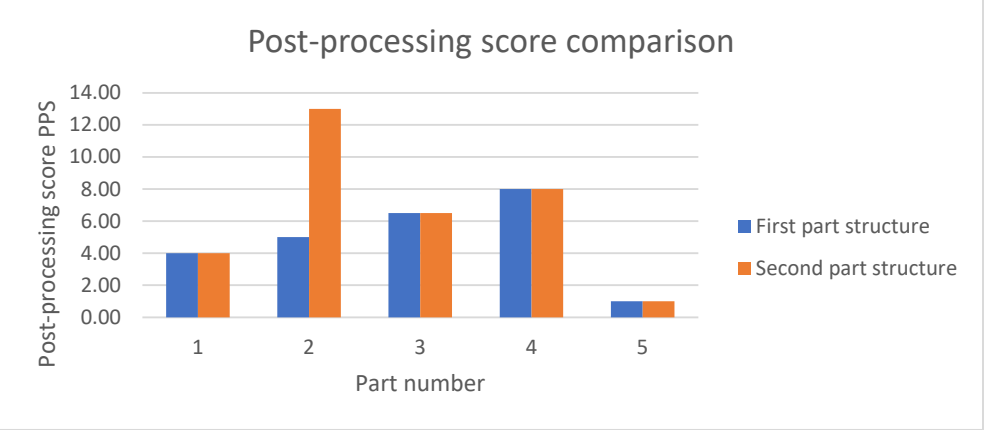


Figure 17. Post-processing score comparison.

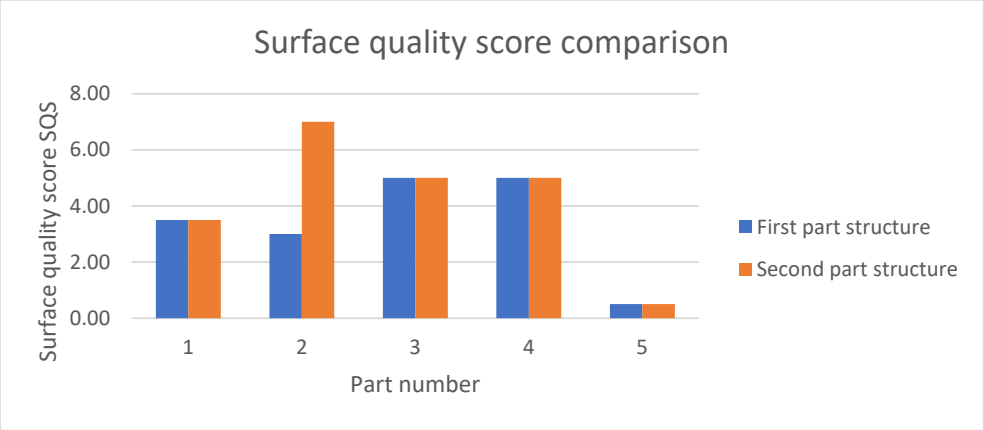


Figure 18. Surface quality score comparison.

By analyzing the experimental data and comparing them to the estimations provided by the slicer at the time of printing process configuration, the following general aspects can be observed:

- The support weight is lower when the part is oriented with the smaller surfaces placed in a position that is close to horizontal, and the larger surfaces placed in a position that is close to vertical.
- The fifth part posture, which is the one provided by the Design for Additive Manufacturing module included in the Siemens NX software (version NX2406), provided the best results (lowest values) for all but one of the analyzed parameters—printing time.
- The arithmetic mean of the SW values is 7.71 for the first structure and 8.58 for the second structure when not including the fifth part posture—experimental data. The arithmetic means for the slicer estimates are 7.35 and 8.04, respectively (also not including the fifth part posture). These values show a greater support weight for the second part structure, but also a lower estimate from the slicer data than the experimental results. The comparative analysis also shows that the largest support requirement was registered for the second part posture. This is the only posture for which an external surface with lattice structure is in direct contact with the supports.
- The arithmetic mean of the TW values is 22.23 for the first structure and 23.69 for the second structure when not including the fifth part posture—experimental data. The arithmetic means for the slicer estimates are 21.97 and 23.44, respectively (also not including the fifth part posture). The values for the part total weight are consistent, especially when taking into account the variations induced by the different support requirements, which is the main factor that influences TW. The lowest TW was observed for the fifth part structure.
- The arithmetic mean of the PD values is 139 for the first structure and 181.5 for the second structure when not including the fifth part posture—experimental data. The arithmetic means for the slicer estimates are 130.5 and 192.5, respectively (also not including the fifth part posture). The second part posture has the lowest print duration, which is correlated to the lowest number of layers. By comparison, the fifth part structure has the highest number of layers and the highest print duration.
- The second part posture has the highest post-processing score. Due to the fact that the supports are in direct contact with a surface having a lattice structure, the complex geometric pattern of the part makes the supports very difficult to remove.
- Also, for the second part, the surface quality score was the highest, mainly for the same reasons described above, as the difficulty of removing the supports affected the quality of the supported surface.

- As a general fact, the surfaces that require support are more likely to have quality issues (since support removal can leave some surplus material attached to the part or it may affect the surface itself). This was noticed on all the printed parts, even for the fifth (optimized) posture. Since the fifth posture required very little support, the PPS and the SQS were much lower than in the other cases.
- Stepping issues affecting curved surfaces were noticed on part postures 1, 3, and 4.

The coefficients for the efficiency score (ES) calculation (a, b, c, d, and e) were determined so that all the parameters included in the formula have the same weight. By analyzing the base values of the experimental data, it can be observed that some parameters have much higher values than others (TW and PD). The objective was to assign the same level of importance for all the analyzed parameters to bring them to the same order of magnitude. In order to achieve this goal, the TW and PD parameters had to be adjusted to the same level as the others. Because the range of the other three parameters was roughly the same, situated between 0.43 and 13, a range between 0 and 15 for the adjusted TW and PD was considered acceptable. Furthermore, in order to ensure that the weight of the parameters was as similar as possible for the calculation, the coefficients were determined so that, when calculating the arithmetic mean for each set of parameters and then multiplying by the corresponding coefficient, the results fall within a range of 0.5 from each other.

Thus, the coefficients were determined using the following procedure:

- SW was chosen as a reference because it was established as the main optimization factor for the study.
- Also, the values for SW, PPS, and SQS have comparable ranges, falling within the same order of magnitude.
- The arithmetic mean for every parameter category multiplied by the corresponding coefficient must fall within a range of a maximum of 0.5 from the arithmetic mean of SW values (since SW was chosen as the reference).
- Thus, for the SW, TW, and PD parameters, the arithmetic means of all the experimental values for both part structures were determined. The values for the fifth part structure were excluded in each case, as these values greatly differ from the others.
- The arithmetic mean of the SW values was calculated at 7.88. The corresponding coefficient a was assigned the value of 1. The value of 7.88 represented the reference value to which all the other arithmetic means (for the other parameter sets) were compared. Thus, the value of 1 was assigned to coefficient a.
- The coefficients for TW and PD were adjusted such as, when applied to the arithmetic mean of these parameters, the results will be as close to the arithmetic mean of the SW values (with a maximum allowed difference of 0.5).
- The arithmetic mean of the TW values was calculated at 22.96. By applying a coefficient of 0.33, it gives a value of 7.65. The value of 0.33 was assigned to the coefficient b.
- The arithmetic mean of the PD values was calculated as 160.25. By applying a coefficient of 0.05, it gives a value of 7.63. The value of 0.05 was assigned to the coefficient c.
- Thus, the coefficients were assigned the following values: a = 1, b = 0.33, c = 0.05, d = 1, e = 1 (since PPS and SQS already have values comparable with those of SW).

Taking into account the considerations presented above, the coefficients and the ES results obtained by applying the formula are illustrated in Table 5.

Table 5. Coefficients and ES results.

First part structure	SW	TW	PD	PPS	SQS	Score
1	6.29	22.14	135	4	3.5	27.60
2	9.91	22.09	107	5	3	30.37
3	3.78	20	147	6.5	5	28.95
4	8.69	24.68	167	8	5	37.87
5	0.54	16.2	185	1	0.5	16.25
Second part structure						
1	8.85	24.83	179	4	3.5	33.15
2	9.94	24.77	171	13	7	46.34
3	5.41	20.36	188	6.5	5	32.65
4	10.15	24.8	188	8	5	40.37
5	0.43	11.23	195	1	0.5	14.96
Arithmetic mean	7.88	22.96	160.25			
Adjusted arithmetic mean	7.88	7.65	7.63			
	a	b	c	d	e	
Coefficients value	1.00	0.33	0.05	1.00	1.00	

5. Conclusions

The research contributes to the field of fused deposition modeling (FDM), focusing on printing posture optimization using the Part Orientation tool from the Design for Additive Manufacturing module included in the Siemens NX software (version NX2406). The main method used for validation was comparative analysis. Two different structure types of the same part were included in the analysis: one with external walls and a conventional infill, and the other with a lattice structure. Thus, the use of the software module could be evaluated for both structures.

The evaluation of the software module efficiency was based on an established set of parameters and a formula that calculates the efficiency score for each printing process. The parameters included in the evaluation were material consumption (expressed through part total weight), support requirements (expressed through support weight), print duration (which is closely linked to productivity), post-processing requirements, and the surface quality of the 3D printed part.

The present study not only determines that certain printing aspects are improved through the use of CAD optimization but also calculates the efficiency of the approach when compared with using more conventional printing postures. Of course, the calculated efficiency score should be considered as dependent on the analysis context, since it relies on the parameters included in the calculation.

The study showed that, taking into account the proposed evaluation parameters, the part printing posture determined through CAD optimization yielded the best results. This solution gave the best output for each parameter except for the print duration. Most notably, the support requirement and total material consumption were minimal.

Because this study was limited to one printer–material profile with a mostly visual surface assessment, in future work we will add quantitative roughness (Ra/Rz/Sa), micro-CT/metallography for porosity, and automated defect detection via computer vision (YOLOv8 on PLA FFF has been shown to be feasible [44]) to tighten the link between orientation, support demand, and defects. Furthermore, as the printing posture influences

the mechanical properties of the part, these characteristics (especially tensile strength) will be analyzed in future research works.

Author Contributions: Methodology, C.A.C.; Validation, A.M.I.; Formal analysis, C.A.C.; Resources, C.A.C.; Data curation, L.F.P.; Writing—original draft, A.M.I.; Writing—review & editing, A.M.I. and L.F.P. All authors have read and agreed to the published version of the manuscript.

Funding: This research received no external funding.

Institutional Review Board Statement: Not applicable.

Informed Consent Statement: Not applicable.

Data Availability Statement: Data is contained within the article.

Conflicts of Interest: The authors declare no conflict of interest.

References

1. Patel, R.; Desai, C.; Kushwah, S.; Mangrola, M.H. A review article on FDM process parameters in 3D printing for composite materials. *Mater. Today* **2022**, *60*, 2162–2166. [CrossRef]
2. Jandyal, A.; Chaturvedi, I.; Wazir, I.; Raina, A.; Ul Haq, M.I. 3D printing—A review of processes, materials and applications in Industry 4.0. *Sustain. Oper. Comput.* **2022**, *3*, 33–42. [CrossRef]
3. Shahrubudin, N.; Lee, T.C.; Ramlan, R. An Overview on 3D Printing Technology: Technological, Materials, and Applications. *Procedia Manuf.* **2019**, *35*, 1286–1296. [CrossRef]
4. Korium, M.S.; Roozbahani, H.; Alizadeh, M.; Perepelkina, S.; Handroos, H. Direct Metal Laser Sintering of Precious Metals for Jewelry Applications: Process Parameter Selection and Microstructure Analysis. *IEEE Access* **2021**, *9*, 126530–126540. [CrossRef]
5. Ishfaq, K.; Abdullah, M.; Mahmood, M.A. A state-of-the-art direct metal laser sintering of Ti6Al4V and AlSi10Mg alloys: Surface roughness, tensile strength, fatigue strength and microstructure. *Opt. Laser Technol.* **2021**, *143*, 107366. [CrossRef]
6. Syrlybayev, D.; Zharylkassyn, B.; Seisekulova, A.; Akhmetov, M.; Perveen, A.; Talamona, D. Optimisation of Strength Properties of FDM Printed Parts—A Critical Review. *Polymers* **2021**, *13*, 1587. [CrossRef] [PubMed]
7. Ngo, T.D.; Kashani, A.; Imbalzano, G.; Nguyen, K.T.Q.; Hui, D. Additive manufacturing (3D printing): A review of materials, methods, applications and challenges. *Compos. Part B Eng.* **2018**, *143*, 172–196. [CrossRef]
8. Blok, L.G.; Longana, M.L.; Yu, H.; Woods, B.K.S. An investigation into 3D printing of fibre reinforced thermoplastic composites. *Addit. Manuf.* **2018**, *22*, 176–186. [CrossRef]
9. Ryan, J.; Dizon, C.; Espera, A.H.; Chen, Q.; Advincula, R.C. Mechanical characterization of 3D-printed polymers. *Addit. Manuf.* **2018**, *20*, 44–67. [CrossRef]
10. Kuznetsov, V.; Solonin, A.; Tavitov, A.; Urzhumtsev, O.; Vakulik, A. Increasing strength of FFF three-dimensional printed parts by influencing on temperature-related parameters of the process. *Rapid Prototyp. J.* **2019**, *26*, 107–121. [CrossRef]
11. Mallikarjuna, B.; Bhargav, P.; Hiremath, S.; Jayachristiyan, K.G.; Jayanth, N. A review on the melt extrusion-based fused deposition modeling (FDM): Background, materials, process parameters and military applications. *Int. J. Interact. Des. Manuf.* **2023**, *19*, 651–665. [CrossRef]
12. Jayanth, N.; Jaswanthraj, K.; Sandeep, S.; Harish Mallaya, N.; Raghul Siddharth, S. Effect of heat treatment on mechanical properties of 3D printed PLA. *J. Mech. Behav. Biomed. Mater.* **2021**, *123*, 104764. [CrossRef]
13. Baechle-Clayton, M.; Loos, E.; Taheri, M.; Taheri, H. Failures and Flaws in Fused Deposition Modeling (FDM) Additively Manufactured Polymers and Composites. *J. Compos. Sci.* **2022**, *6*, 202. [CrossRef]
14. Gibson, I.; Rosen, D.; Stucker, B.; Khorasani, M. *Additive Manufacturing Technologies*; Springer: Cham, Switzerland, 2020.
15. Tofail, S.A.M.; Koumoulos, E.P.; Bandyopadhyay, A.; Bose, S.; O'Donoghue, L.; Charitidis, C. Additive manufacturing: Scientific and technological challenges, market uptake and opportunities. *Mater. Today* **2018**, *1*, 1–16. [CrossRef]
16. Aloyaydi, B.; Sivasankaran, S.; Mustafa, A. Investigation of infill-patterns on mechanical response of 3D printed poly-lactic-acid. *Polym. Test.* **2020**, *87*, 106557. [CrossRef]
17. Bakır, A.A.; Atik, R.; Özerinç, S. Effect of fused deposition modeling process parameters on the mechanical properties of recycled polyethylene terephthalate parts. *J. Appl. Polym. Sci.* **2020**, *138*, 49709. [CrossRef]
18. Tang, C.; Liu, J.; Yang, Y.; Liu, Y.; Jiang, S.; Hao, W. Effect of process parameters on mechanical properties of 3D printed PLA lattice structures. *Compos. Part C Open Access* **2020**, *3*, 100076. [CrossRef]
19. Jatti, V.S.; Sapre, M.S.; Jatti, A.V.; Khedkar, N.K.; Jatti, V.S. Mechanical Properties of 3D-Printed Components Using Fused Deposition Modeling: Optimization Using the Desirability Approach and Machine Learning Regressor. *Appl. Syst. Innov.* **2022**, *5*, 112. [CrossRef]

20. Kantaros, A.; Piromalis, D. Employing a Low-Cost Desktop 3D Printer: Challenges, and How to Overcome Them by Tuning Key Process Parameters. *Int. J. Mech. Appl.* **2021**, *10*, 11–19. [CrossRef]
21. Gao, G.; Xu, F.; Xu, J.; Tang, G.; Liu, Z. A Survey of the Influence of Process Parameters on Mechanical Properties of Fused Deposition Modeling Parts. *Micromachines* **2022**, *13*, 553. [CrossRef] [PubMed]
22. Giri, J.; Chiwande, A.; Gupta, Y.; Mahatme, C.; Giri, P. Effect of process parameters on mechanical properties of 3d printed samples using FDM process. *Mater. Today Proc.* **2021**, *47*, 5856–5861. [CrossRef]
23. Raju, M.; Gupta, M.K.; Bhanot, N.; Sharma, V.S. A hybrid PSO-BFO evolutionary algorithm for optimization of fused deposition modelling process parameters. *J. Intell. Manuf.* **2019**, *30*, 2743–2758. [CrossRef]
24. Górski, F.; Wichniarek, R.; Kuczko, W.; Andrzejewski, J. Experimental determination of critical orientation of abs parts manufactured using fused deposition modelling technology. *J. Mach. Eng.* **2015**, *15*, 121–132.
25. Hernandez, R.; Slaughter, D.; Whaley, D.; Tate, J.; Asiabanpour, B. Analyzing the tensile, compressive, and flexural properties of 3d printed abs p430 plastic based on printing orientation using fused deposition modeling. In Proceedings of the 27th Annual International Solid Freeform Fabrication Symposium, Austin, TX, USA, 12–14 August 2019. Available online: https://hdl.handle.net/2152/89645 (accessed on 23 April 2024).
26. Wang, X. Natural frequency optimization of 3D printed variable–density honeycomb structure via a homogenization–based approach. *Addit. Manuf.* **2017**, *20*, 189–198. [CrossRef]
27. Nguyen, C.H.P.; Kim, Y.; Choi, Y. Design for Additive Manufacturing of Functionally Graded Lattice Structures: A Design Method with Process Induced Anisotropy Consideration. *Int. J. Precis. Eng. Manuf.-Green Technol.* **2021**, *8*, 29–45. [CrossRef]
28. Gibson, L.J.; Ashby, M.F. *Cellular Solids: Structure and Properties*; Cambridge Solid State Science Series; Cambridge University Press: Cambridge, UK, 1997.
29. McGregor, D.J.; Tawfick, S.; King, W.P. Mechanical properties of hexagonal lattice structures fabricated using continuous liquid interface production additive manufacturing. *Addit. Manuf.* **2019**, *25*, 10–18. [CrossRef]
30. Zisopol, D.G.; Tănase, M.; Portoacă, A.I. Innovative Strategies for Technical-Economical Optimization of FDM Production. *Polymers* **2023**, *15*, 3787. [CrossRef] [PubMed]
31. Jackson, B.; Fouladi, K.; Eslami, B. Multi-Parameter Optimization of 3D Printing Condition for Enhanced Quality and Strength. *Polymers* **2022**, *14*, 1586. [CrossRef]
32. El youbi El idrissi, M.A.; Laaouina, L.; Jeghal, A.; Tairi, H.; Zaki, M. Modeling of Energy Consumption and Print Time for FDM 3D Printing Using Multilayer Perceptron Network. *J. Manuf. Mater. Process.* **2023**, *7*, 128. [CrossRef]
33. 3DiM Benchmark. Available online: https://www.kaggle.com/dataset/c22f9996866156344599fd5baf48aaa8ac8ccce9a849b050ceeea36ba4e9c8f9 (accessed on 25 June 2022).
34. Yang, Y.; Yang, B.; Chang, Z.; Duan, J.; Chen, W. Research Status of and Prospects for 3D Printing for Continuous Fiber-Reinforced Thermoplastic Composites. *Polymers* **2023**, *15*, 3653. [CrossRef]
35. Li, N.; Guido, L.; John, J.; Morais Manuel, V.C.; Frank, H. Microwave additive manufacturing of continuous carbon fibers reinforced thermoplastic composites: Characterization, analysis, and properties. *Addit. Manuf.* **2021**, *44*, 102035. [CrossRef]
36. Liu, H.; Lin, D.; Yang, L.; Wu, S.; Ren, Y.; Xiong, R.; Leng, S.; Seop Kim, H.; Yan, C.; Shi, Y. Enhanced mechanical responses and fatigue behaviors of triply periodic minimal surface lattice metamaterials by twin-oriented lattice design. *Int. J. Fatigue* **2025**, *201*, 109172. [CrossRef]
37. Numan, K.; Aniello, R. A systematic review of design for additive manufacturing of aerospace lattice structures: Current trends and future directions. *Prog. Aerosp. Sci.* **2024**, *149*, 101021. [CrossRef]
38. Min, K.-E.; Jang, J.-W.; Shin, J.; Kim, C.; Yi, S. Development of Prediction Method for Dimensional Stability of 3D-Printed Objects. *Appl. Sci.* **2023**, *13*, 11027. [CrossRef]
39. Bassoli, E.; Defanti, S.; Tognoli, E.; Vincenzi, N.; Degli Esposti, L. Design for Additive Manufacturing and for Machining in the Automotive Field. *Appl. Sci.* **2021**, *11*, 7559. [CrossRef]
40. Safali, S.; Berk, T.; Makelov, B.; Acar, M.A.; Gueorguiev, B.; Pape, H.-C. The Possibilities of Personalized 3D Printed Implants—A Case Series Study. *Medicina* **2023**, *59*, 249. [CrossRef]
41. Cavallo, L.; Marcianò, A.; Cicciù, M.; Oteri, G. 3D Printing beyond Dentistry during COVID 19 Epidemic: A Technical Note for Producing Connectors to Breathing Devices. *Prosthesis* **2020**, *2*, 46–52. [CrossRef]
42. Simion, I.; Arion, A. Dimensioning rules for 3D printed parts using additive technologies (FDM). *U.P.B. Sci. Bull. Ser. D* **2016**, *78*, 79–92.
43. PolyTerraTM PLA Technical Data Sheet. Available online: https://c.cdnmp.net/490505258/custom/prod/1_fisa_tehnica_2517.pdf?rv=1695896359 (accessed on 5 January 2024).
44. Talanga, A.; Hadar, A.; Dragoi, M.V.; Nisipeanu, I.; Ali, H.A.; Suciu, C. YOLO-v8 in capturing imperfections generated by changing 3D printer parameters. *U.P.B. Sci. Bull. Ser. C* **2024**, *86*, 253–266.

Disclaimer/Publisher's Note: The statements, opinions and data contained in all publications are solely those of the individual author(s) and contributor(s) and not of MDPI and/or the editor(s). MDPI and/or the editor(s) disclaim responsibility for any injury to people or property resulting from any ideas, methods, instructions or products referred to in the content.